



Evaluate the impact of a 4-hour tandem phase on the continuity of nadir altimetry measurements between S3 and S3NG-T

Noémie Lalau¹, Michaël Ablain¹, Thomas Vaujour¹, François Boy², Gerald Dibarboure², and Alejandro Egido³

¹MAGELLIUM, Ramonville Saint-Agne, 31520, France

²CNES, Toulouse, 31400, France

³ESA, ESTEC, Noordwijk, 2201 AZ, The Netherlands

Correspondence: Noémie Lalau (noemie.lalau@magellium.fr)

Abstract. The upcoming Sentinel-3 Next Generation Topography (S3NG-T) mission, designed to succeed the current Sentinel-3 (S3) mission, will operate on the same ground tracks as the current S3 constellation to maximise continuity of measurements, but with a fixed 4-hour temporal lag due to satellite design constraints. This configuration prevents the implementation of a classical near-simultaneous tandem phase, traditionally used for inter-mission cross-calibration, and raises concerns regarding 5 the impact of short-term oceanic variability on continuity assessment.

In this study, we evaluate the feasibility and expected performance of a 4-hour delayed tandem phase for cross-calibrating S3 and S3NG-T. Using tandem datasets from Sentinel-3A/B and Jason-3/Sentinel-6 missions, combined with SWOT KaRIn observations, we develop a methodology to quantify the oceanic variability introduced by a 4-hour delay and to evaluate its effect on the accuracy of inter-mission offset estimates.

10 Results indicate that the classical tandem configuration achieves regional offset uncertainties of approximately 2 mm over a three-month period. In contrast, a 4-hour delayed tandem phase increases this uncertainty to about 7 mm in the same period, but still performs significantly better than non-tandem scenarios. Extending the 4-hour tandem phase to one year enables the detection of systematic errors of ± 3.5 mm amplitude, sufficient to ensure continuity between S3 and S3NG-T. These findings demonstrate that, despite additional oceanic variability, a 4-hour tandem configuration remains a viable and effective strategy 15 for cross-calibration, especially when supported by improved environmental corrections and extended observation duration.

1 Introduction

The Sentinel-3 (S3) and Sentinel-3 Next Generation Topography (S3NG-T) missions are part of the Copernicus Programme led by the European Commission. The European Space Agency (ESA), is mandated to define the Copernicus space component (CSC) architecture based on user requirements coordinated by the Commission, in collaboration with EUMETSAT, 20 and Member States. The S3 and S3NG-T missions aim at providing continuous, high-accuracy measurements of sea surface topography, sea and land surface temperature, and ocean and land surface colour. S3 plays a central role in supporting operational oceanography, environmental monitoring, and long-term climate records. Looking ahead to the 2030–2050 timeframe,



the S3NG-T mission primary objective is to ensure the continuity of the existing Copernicus S3 nadir-altimeter measurements with enhanced performance, coverage and revisit time (European Space Agency, 2025).

25 The S3NG-T mission consists of two large spacecrafts equipped with an across-track interferometer swath altimeter (SAOOH), a synthetic aperture radar (SAR) nadir altimeter (Poseidon-5), a multi-channel microwave radiometer, and a precise orbit determination suite. The two spacecrafts will fly in a sun-synchronous orbit at 6pm local time ascending node (LTAN), at a mean orbital height of 815 km, with an orbital phase difference of 140°, achieving an interleaved ground-track between both satellites, and matching the Sentinel3A/3B ground tracks. Since S3NG-T satellites will be of a new design, it is imperative that the
30 characteristics of the new system are introduced into the S3 time series in a manner that does not introduce instability into the long time series.

To achieve the primary objective of ensuring the continuity of S3 topographic measurements, it is essential to have a successful cross-calibration between the current S3 constellation and the S3NG-T mission. The most effective method for accurately assessing continuity between successive altimeter missions over the ocean is the tandem flight phase (hereafter referred to as
35 'tandem phase'). Tandem phases have been systematically implemented following the launch of new reference altimetry missions, including TOPEX-Poseidon and Jason-1 (2002), Jason-1 and Jason-2 (2008), Jason-2 and Jason-3 (2016), and Jason-3 and Sentinel-6 Michael Freilich (2021-2022). They have also been used between non-reference missions, such as ERS-2 / Envisat (2007-2008, 2010-2011) and Sentinel-3A and Sentinel-3B (2018). This S3A/B tandem phase allowed a precise cross-calibration of the S3 constellation instruments (Rieu et al., 2021), supporting the generation of consistent and unbiased time-
40 series observations for climate monitoring (Clerc et al., 2020), following the approach previously applied to the Jason series (Dibarbour et al., 2011). During a tandem phase, two successive missions follow an identical ground track at intervals of less than one minute. These calibration campaigns are essential for maintaining the accuracy and stability of the satellite altimetry record (Dorandeu et al., 2004; LEULIETTE et al., 2004; Zawadzki and Ablain, 2016). The significant benefits of a tandem phase have been thoroughly explained by Ablain et al. (2025). A key assumption during this period is that the ocean and
45 atmospheric conditions, at the scales of interest, do not vary significantly between measurements made by the two altimetry missions. This allows for the cancellation of geophysical and atmospheric effects when comparing sea level measurements from the two altimeters. Consequently, the relative errors between altimetry missions, arising from instrumental differences (e.g., altimeter noise), data processing disparities (e.g., retracking algorithms), precise orbit determination, and variations in the mean sea surface, can be accurately determined. Averaging these differences over the entire tandem phase period enables
50 cancellation of random effects, thereby allowing for the accurate determination of systematic instrumental errors between the two successive altimetry missions (Masters et al., 2012; Henry et al., 2014; Guérou et al., 2023).

The precise determination of these systematic sea level differences due to instrumental errors facilitates investigation of their origin and potential future correction. Furthermore, averaging these systematic sea level differences provides the mean sea level offset between two successive missions. This offset is essential for accurately linking the two successive altimeter
55 missions, thereby ensuring a continuous sea level data record.

On the global scale, the mean sea level offset between two successive reference missions is calculated with an accuracy lower than 0.5 mm at a confidence level of 68% (Zawadzki and Ablain, 2016; Guérou et al., 2023). At regional scales of a few



hundred km, the uncertainty of the mean sea level offset increases to 2 mm (update from Prandi et al. (2021)) depending on the area. These uncertainty levels, obtained during the tandem phase, demonstrate our ability to assess the sea level continuity on 60 both global and regional scales between two successive altimetry missions, and represent the limit of detectability of systematic errors.

However, the standard tandem phase with a near-zero temporal lag will not be feasible between S3 and S3NG-T due to orbital constraint, with a 6:00 p.m. LTAN for S3NG-T and 10:00 p.m. LTAN for S3A/B. This configuration imposes a 4-hour time lag between the S3 and S3NG-T observations at the same location. As a result, the two altimeters will no longer observe 65 the same oceanic surface simultaneously during their tandem phase. Even when spatially collocated, sea level measurements taken just four hours apart will differ significantly due to natural, high-frequency ocean processes. These include internal tides, internal waves, inertial motions, mesoscale eddies, and submesoscale dynamics, all of which induce significant fluctuations on sub-daily timescales (Dufau et al., 2016; Cronin, M. et al., 2012). As a consequence, the introduction of ocean variability effects in the sea level differences calculated during a 4-hour tandem phase will reduce our ability to assess the sea level 70 continuity between S3 and S3NG.

This study aims to evaluate the impact of a 4-hour tandem phase on the continuity of sea level measurements provided between S3 and S3NG-T nadir altimetry measurements. To achieve this objective, we explore methods for quantifying the oceanic variability introduced by this 4-hour delay and evaluate potential strategies to ensure reliable continuity in the absence of a conventional tandem phase. The datasets used in this study are detailed in Section 2. Section 3.1 presents the method used 75 to verify continuity and section 3.2 presents the methodology developed to quantify the uncertainty associated. Section 3.3 describes the approach adopted to characterise the oceanic variability induced by the 4-hour lag. The main results are presented in Section 4, and additional comparisons with other methods and missions are discussed in Section 5.

2 Data

This study relies on altimetric missions with overlapping temporal coverage to evaluate tandem phases and quantify their 80 impact on inter-mission continuity. The primary missions considered include Jason-3 (J3), Sentinel-6 Michael Freilich (S6A), Sentinel-3A (S3A), Sentinel-3B (S3B), and SWOT. These missions provide complementary datasets across different orbits and tandem configurations.

The tandem phase between S3A and S3B serves as a proxy for the future configuration of Sentinel-3D and S3NG. This phase represents a relevant case study of two satellites flying on the Sentinel-3 orbit and constitutes the core dataset from 85 which the main results of this study are derived. The S3A/S3B tandem phase lasted from 7 June to 16 October 2018, spanning four complete 27-day cycles or ten 12-day sub-cycles (Clerc et al., 2020).

For comparison, data from the J3 and S6A missions were used to analyse a longer tandem phase on a different orbit, enabling an application of the methodology beyond the Sentinel-3 constellation. The J3/S6A tandem phase extended from 17 December 2020 to 7 April 2022 and includes more than 40 cycles of 10 days. However, due to an anomaly on the Poseidon-4 altimeter



90 (side A) shortly after the S6A launch, only the data acquired after the switch to side B -performed on 14 September 2021- were retained for this study (Dinardo et al., 2022).

In addition, SWOT KaRIn data were used to estimate the impact of natural oceanic variability on SLA differences over a 4-hour time lag. SWOT was selected due to its dense network of crossover points with the S3A and S3B ground tracks, offering high spatial and temporal resolution, which is essential for characterising oceanic variability effects.

95 The data used in this study are publicly available. We employed L2P 2024 products for J3, S6A, S3A, and S3B, and the SWOT KaRIn Science Phase data (Version 1.0.2). The SWOT Level-3 Low Rate SSH product -derived from the KaRIn L2 low-rate ocean data- is produced by the AVISO and DUACS teams as part of the DESMOS Science Team project and is freely accessible via AVISO (AVISO/DUACS, 2024).

100 The L2P contain the along-track sea level anomaly at 1Hz (SLA, see Eq. 1) calculated after applying a validation process fully described in the product handbook of each altimetry mission (Along-track Level-2+ (L2P) Sea Level Anomaly Sentinel-3 / Jason-CS-Sentinel-6 Product Handbook, 2022). The along-track SLA is derived from the following equation:

$$SLA = Orbit - Range - \sum_i Correction_i - Mean\ Sea\ Surface \quad (1)$$

105 where *Orbit* is the radial distance between the satellites and the geoid, *Range* the distance between the satellite and the sea surface, $\sum_i Correction_i$ are the sum of the geophysical and atmospheric corrections to be applied (e.g. ocean, polar and earth tides, wet and dry troposphere corrections, sea state bias correction,...), *Mean Sea Surface* is the mean of the sea surface height from which sea level anomalies are derived. The geophysical corrections applied in L2P products for the SLA calculation are already homogenised for each altimetry mission and identical during a tandem phase.

3 Methods

3.1 Comparison between two missions

110 To evaluate the continuity of sea level measurements between two altimetric missions, we investigate in this study three distinct scenarios. The first is the classical tandem phase, in which the satellites follow each other closely in both space and time, allowing for nearly simultaneous co-located observations. The second scenario considers a configuration without any tandem phase, where sea level data from the two missions are neither co-located in time nor space. The third scenario simulates a delayed tandem phase with a 4-hour temporal offset, where measurements are co-located in space but not in time (4-hour time lag). Each of these configurations presents different conditions for estimating the offset between missions, and consequently different associated uncertainties. By comparing the uncertainty in sea level differences across these three scenarios, we aim to assess the feasibility and accuracy of the 4-hour tandem phase as a substitute for the classical approach.

115 The method used to verify continuity is applicable to both tandem and non-tandem scenarios. For each cycle of each mission, along-track SLA data are aggregated onto a regular spatial grid to produce gridded fields of mean sea level (MSL). These gridded fields, referred to as regional MSL grids, are constructed for each cycle (or subcycle in the case of S3) independently.



To homogenize comparisons between missions with different orbital characteristics, a consistent temporal window of 12 days -corresponding to three 4-day sub-cycles of the S3A/S3B orbit- was adopted for all configurations. This allows direct comparison between the 10-day cycles of J3/S6A and the 27-day cycles of S3A/S3B.

125 To ensure consistency in spatial resolution and optimise coverage, SLA data are binned into grid cells of $3^\circ \times 3^\circ$. This resolution minimises the number of empty cells, particularly when considering 12-day subcycles for S3A and S3B. This 3° grid spacing is uniformly adopted in all scenarios and missions in this study.

130 For each cycle, the difference between the regional MSL grids from the two missions is computed, resulting in a series of SLA difference maps. By taking a weighted spatial average of each difference map, we obtain a time series of global mean sea level (GMSL) differences between the two missions, with one value per cycle. The mean of this time series provides an estimate of the global offset.

In addition to this global assessment, regional offsets are also evaluated. In each grid cell, a time series of SLA differences is derived across the observation period. The temporal average of this time series yields a map of the regional offsets. This spatially resolved approach allows for the assessment of geographic variability in the offset and is particularly useful for analysing the effect of spatially dependent phenomena, such as instrument biases (Nilsson et al., 2022).

135 In this study, the focus is placed primarily on regional offset estimation and its uncertainty. On a global scale, the impact of a 4-hour time lag is negligible due to the averaging of uncorrelated oceanic signals. However, at regional scales, such variability can introduce significant errors, making regional analyses crucial to understand the implications of the 4-hour tandem configuration.

3.2 Uncertainty computation

140 Quantifying the uncertainty associated with regional MSL (RMSL) offset estimates is essential for assessing the reliability of continuity verification methods. This uncertainty reflects the variability of differences observed across several repeat cycles and is evaluated separately for each of the three continuity scenarios described above. In this study, we consider two complementary approaches to quantify the uncertainty of regional offset estimates. The first method provides a single global uncertainty value based on the spatial variability of the regional offset map, offering an integrated view of the spatial dispersion in offset estimates.

145 The second method estimates uncertainty locally at each grid point by analysing the temporal variability of SLA differences, while also accounting for potential autocorrelation in the time series. These two methods offer distinct yet complementary perspectives -spatial versus temporal- and together provide a more robust and comprehensive assessment of uncertainty under varying observational configurations.

3.2.1 Spatial standard deviation of RMSL offset maps

The method described in Section 3.1 for comparing missions produces a map of RMSL differences for each cycle. The temporal mean of these cycle-by-cycle differences is then computed for each grid cell. This temporal average, $\Delta MSL(lat, lon)_{n_cycle}$, represents the RMSL offset between the two missions over "n" cycles. This average can be computed during or outside the tandem phase. The uncertainty associated with the RMSL offset is then quantified as the standard deviation of the spatial



variations of this temporal mean. This standard deviation, denoted as

$$u = \sigma(\Delta MSL(lat, lon)_{n_cycle})$$

150 provides an estimate of the RMSL offset uncertainty relative to the global mean. The uncertainty derived from this methodology assumes that the RMSL differences represent N independent realizations of the offset error. By verifying that the distribution of these differences follows a Gaussian distribution, the standard deviation can be interpreted as a $1-\sigma$ uncertainty. To ensure this estimate is realistic, it is crucial to correct for any detectable systematic effects before performing the calculations. Uncorrected systematic errors could inflate the standard deviation, leading to an overestimation of the uncertainty.

155 **3.2.2 Regional offset uncertainty**

Another way to calculate the uncertainty of the RMSL offset is to compute the standard deviation of each temporal time series of MSL at regional scales, as proposed by Prandi et al. (2021):

$$\sigma(lat, lon)_{n_cycle} = \sigma(\Delta MSL_{lat, lon}(t))$$

The uncertainty for each grid cell is then computed using the formula from Guérou et al. (2023):

$$u = t_{1-\alpha/2}^{n-1} \frac{\sigma_{lon, lat}}{\sqrt{n'}} \quad (2)$$

and

$$n' = \frac{1 - \rho_1}{1 + \rho_1} n_{sample} \quad (3)$$

160 Where σ is the standard deviation of the sample ; n is the number of measurements ; t is the Student's coefficient for $(n - 1)$ degrees of freedom and a confidence level of α ; n' is the effective sample size, accounting for any autocorrelation in the data.

Unlike the previous approach, which estimates a single regional offset uncertainty relative to the global mean, this method calculates the uncertainty of each local offset. However, for this study, the small sample size during the tandem phase limits the accuracy of n' .

165 **3.3 Accounting for 4-hour variability**

To quantify the variance of oceanic variability and measurement errors over short time intervals, we analysed crossover differences between SWOT's KaRIn swath data and Sentinel-3A/3B nadir data (Δ SSHA). This analysis is based on almost one year of data from SWOT's science phase, leveraging a high number of crossovers and an extensive spatial coverage. A crossover is defined as the intersection of ground tracks from two satellites, enabling the comparison of spatially colocated measurements, 170 although acquired at different times.

3.3.1 Estimation of 4-hour variability

The first step involves constructing a map of Δ SSHA variance for crossovers with time interval of $\Delta t = 4$ hours, using data aggregated into $5^\circ \times 5^\circ$ grid cells. This map captures high-frequency oceanic variability, systematic errors, and altimeter noise,



represented as: $\sigma^2 = \sigma_{ocean}^2 + \sigma_{SWOT}^2 + \sigma_{S3}^2$ where σ_{ocean}^2 accounts for oceanic variability and $\sigma_{SWOT}^2, \sigma_{S3}^2$ represent
175 the systematic errors and instrumental noise for SWOT and Sentinel-3, respectively.

The second step consists of generating a variance map for Δt approaching 0 hours, where the contribution of oceanic variability is negligible. This map isolates systematic errors and altimeter noise in the $\Delta SSHA$ measurements, providing a baseline against which to compare the 4-hour map. Both maps are processed using a mean filter followed by interpolation to fill data gaps and oversampling to a finer $3^\circ \times 3^\circ$ resolution. By subtracting the 0-hour variance map from the 4-hour variance map,
180 an upper bound on the variance associated with 4-hour oceanic variability is obtained. This estimate constitutes an upper bound because the calculation may still include residual instrumental and environmental correction errors. The variance associated with altimeter noise is assumed to be time-invariant and therefore cancels out in the subtraction. The resulting variance map is expressed in terms of $\sigma_{i,j}^2$, representing the variance within each $3^\circ \times 3^\circ$ grid cell. This map reveals spatial heterogeneities in the variance of $\Delta SSHA$. Notable high values are observed in regions such as the Madagascar Basin and the Indonesian
185 archipelago (see Fig. A2).

3.3.2 Propagation of variability into offset uncertainty

To simulate the impact of additional sea-level variance due to a 4-hour tandem phase, random error grids are introduced into the observed SSHA differences during the tandem phase. The $3^\circ \times 3^\circ$ grid variance map is used to generate regional random error grids. For each cycle, a random error grid is constructed following a normal distribution with variance $\sigma_{i,j}$. These regional
190 error grids are then added to the observed SSHA differences during the tandem phase of Sentinel-3A and Sentinel-3B. The offset uncertainty is then computed on this new dataset applying the same methodology as described in Section 3.2.

4 Results: Classic tandem vs. 4-hour tandem phase

In this section, we compare the continuity performance of three configurations: the classical S3A/S3B tandem phase, a 4-hour delayed tandem configuration, and a non-tandem scenario. The analysis is conducted using along-track comparison methods
195 over a $3^\circ \times 3^\circ$ grid with 12-day sub-cycles, as described in Section 3.1. As shown in Fig. 1, over a period of ten 12-day cycles (approximately four months), the regional inter-mission bias uncertainty is estimated at 2 mm in the classical tandem phase, compared to 7 mm for the 4-hour delayed tandem and 10.5 mm in the non-tandem scenario -representing three and five times higher uncertainty, respectively.

These results underscore the advantage of close spatiotemporal co-location in reducing the measurement noise and improving
200 the inter-mission bias precision. As expected, the uncertainty in the bias estimate decreases with the number of tandem cycles, primarily due to the averaging of random errors. The tandem phase also enables a more effective detection of systematic errors, as the oceanic variability is minimized. These systematic errors are visible on the regional offset map during the tandem phase (see Fig. A1), but they are noisier with a 4-hour delay. In the non-tandem configuration, these same systematic patterns begin to emerge only after one year of observation, with amplitudes reaching up to 6 mm.



205 While the 4-hour temporal lag introduces additional variability, the resulting uncertainty remains significantly lower than in the absence of any tandem overlap. This demonstrates that even partial co-location -such as with a few hours of delay- can significantly improve the reliability of continuity assessments.

5 Assessment

210 This section evaluates the robustness and general applicability of the proposed continuity assessment framework. Specifically, we investigate three complementary aspects: (1) the consistency of results when applied to a different pair of altimetric missions, namely J3 and S6A; (2) the sensitivity of the along-track comparison methodology, evaluated through comparison with a crossover-based approach; and (3) the consistency of regional uncertainty estimates obtained from two distinct statistical methods. Together, these analyses allow us to test the validity, flexibility, and limitations of the proposed methodology under varying mission configurations and observational constraints.

215 5.1 Comparison with J3/S6A missions

220 To validate the robustness of our findings, we performed a comparative analysis using J3 and S6A missions (see Fig. 2), which are on a different orbit than S3A and S3B. These two missions also benefited from a tandem phase, offering an opportunity to verify the performance observed with the S3A/S3B configuration. Results confirm that orbital characteristics do not significantly affect the ability to detect inter-mission offsets during tandem phases, thereby validating the method across different mission pairs.

225 Outside the tandem phase, however, the orbital configuration becomes a critical factor. After one year of data, the uncertainty ranges from 6 mm for S3A/S3B to 12 mm for J3/S6A. The reference mission orbit (used by TOPEX, the Jason series, and S6A) has a 9.9-day repeat cycle and a ground track separation of 314 km at the equator. In a two-satellite configuration -such as J3 and S6A, where J3 is placed on an interleaved orbit following the tandem phase-, the inter-track separation at the equator is reduced from 314 km to 157 km after one full cycle. For S3A/S3B's configuration, this separation is reduced from 104 km to 52 km, reducing the impact of oceanic variability. The offset uncertainty observed in these non-tandem conditions is highly sensitive to such geometric configurations.

5.2 Sensitivity Analysis of the Along-Track Method: Comparison with Crossover-Based Approach

230 To assess the sensitivity and robustness of the along-track comparison methodology, we conducted a parallel analysis using a second method based on crossovers between the two altimetric missions (see Fig. 2).

The crossover-based method aggregates SLA difference values at these points for time lags below 10 days. This upper limit was chosen to ensure sufficient spatial coverage and data volume for statistically meaningful results. The differences are spatially averaged into $3^\circ \times 3^\circ$ grid cells, resulting in gridded MSL difference fields analogous to those derived from along-track comparisons. The regional offset is then estimated by averaging the time series of each cell across multiple cycles.



235 A key advantage of the crossover-based approach lies in its relative independence from the specific orbital configuration or tandem scenario. The method provides consistent results across different mission pairs, such as J3/S6A and S3A/S3B. This robustness to orbital configuration enhances the general applicability of the crossover technique and reinforces its relevance as a complementary method for altimetric continuity assessments. Over a one-year timescale, both configurations yield an uncertainty of approximately 6 mm, closely matching the results obtained outside the tandem phase for S3A/S3B.

240 **5.3 Comparison of two uncertainty estimation methods**

To further assess the consistency of uncertainty estimates, we apply both statistical methods described in Section 3.2 to a longer tandem phase available with the J3/S6A mission dataset. The two methods for estimating regional offset uncertainty each offer distinct advantages and are suited for different purposes, depending on the available data and the objectives of the analysis.

245 The first method, based on the spatial standard deviation of the regional offset field, is particularly well-suited when only a limited number of cycles are available. It allows for a rapid estimation of regional offset uncertainty and serves as an independent validation approach. Its simplicity and minimal data requirements make it especially useful for short-duration tandem phases or initial assessments. It is however sensitive to uncorrected systematic errors that could lead to an overestimation of the uncertainty.

250 The second method estimates uncertainty at the local scale by analysing the temporal variability of SLA differences within each grid cell. This approach aligns with global uncertainty assessment analyses, ensuring consistency between regional and global uncertainty assessments. One of its major advantages is the ability to produce spatially resolved uncertainty maps, facilitating the construction of detailed regional uncertainty budgets and enabling identification of geographically heterogeneous behaviours. Additionally, this method is less sensitive to systematic error corrections performed beforehand. By explicitly accounting for potential autocorrelation through the calculation of an effective sample size, this approach provides a more 255 rigorous statistical interpretation. However, its reliability is constrained by the number of available cycles, particularly in short tandem phases.

Together, these two complementary uncertainty estimation approaches provide consistent results and improve confidence in the robustness of the continuity assessment framework. A comparative summary of both methods is presented in Fig. 3.

6 Conclusions

260 This study addresses the critical issue of ensuring continuity in SLA measurements between successive S3 and S3NG-T altimetry missions. Traditional tandem phase, where missions fly in close formation, are crucial for mission continuity. However, orbital constraints prevent a classic tandem phase between S3 and S3NG-T, necessitating a new approach with a 4-hour time delay between observations. The introduction of this 4-hour delay brings an additional source of uncertainty in offset estimation. Quantifying this uncertainty is essential to evaluate the feasibility and effectiveness of such a configuration for maintaining data 265 continuity. In this study, we developed a technique to simulate the 4-hour delay using crossovers with SWOT KaRIn data and assessed its impact by comparing multiple configurations, including scenarios with and without tandem phase, as well as differ-



ent spatial and temporal sampling schemes. By analysing nearly one year of observations and implementing tailored statistical metrics, we quantified the continuity of SLA measurements between two missions and estimated the associated uncertainties. Beyond the methodological aspects, these findings have significant implications for ocean science and climate applications
270 requiring long-term and stable satellite sea level data records. Our results demonstrate that sea level data continuity between S3 and S3NG-T is maintained despite a 4-hour delay instead of a classical near-simultaneous calibration phase. Although this 4-hour delay introduces short-term time-correlated effects due to ocean variability, we show that such effects can be effectively quantified and mitigated through extended calibration period.

Specifically, while classic tandem configurations can achieve a 2 mm detectability threshold within three months, a 4-
275 hour tandem phase would require approximately two years of continuous observations to reach a similar level of calibration precision (Fig. 4). However, the demonstrated ability to detect systematic differences of ± 3.5 mm within one year highlights the feasibility of this approach. Consequently, the methodology developed ensures for users that future S3NG-T datasets will remain seamless and consistent with the existing S3 legacy, given the possibility of extending the tandem phase to one year.

Although this study focuses on SLA, the methodology is equally applicable to other key altimetric parameters such as
280 significant wave height (SWH) and backscatter coefficient (σ_0). Since the primary objective of S3NG-T is to ensure the continuity of S3 measurements across all topographic products -ocean, inland water (rivers and lakes), sea ice, ice sheets, and atmospheric parameters- the approach developed here holds broad relevance. In addition, the study design supports regional analyses, allowing targeted assessments in specific ocean basins or geographic areas of interest.

A key limitation of the method developed in this study is that SSHA differences at a 4-hour time lag reflect the combined effects of oceanic variability and altimetric measurement errors. These errors arise from multiple sources, including inaccuracies in environmental corrections such as ocean tides, atmospheric influences, and internal tide signals. Nonetheless, anticipated improvements in altimetric data processing and environmental modeling over the next decade -such as enhanced tide models leveraging SWOT's high-resolution observations (Zhao, 2024)- are expected to significantly reduce these sources of uncertainty. As a result, future comparisons between S3NG-T and S3 will benefit from these advancements, enabling more precise
290 assessments of mission continuity. An important perspective of this study is then the potential to isolate and quantify the respective contributions of oceanic variability and measurement errors to the overall uncertainty in SLA differences during a 4-hour tandem phase. Achieving such a separation would enable a more robust estimation of offset uncertainties and offer valuable insights into the nature and sources of altimetric errors.

Author contributions. N.L and M.A conceived the presented approach. N.L., M.A. and T.V. developed the theory and performed the computations.
295 All authors discussed the results and contributed to the final manuscript.

Competing interests. None declared



Acknowledgements. This study was initiated as part of the S3NGT-MPUA project, supported by ESA. It also benefited from initial funding by CNES to develop the study's core concept. Additionally, the ASELSU project, also supported by ESA, contributed to improving the formalism used in this article to provide uncertainty estimates. All computational resources, including the use of specific libraries and data access, were facilitated by access to the CNES HPC cluster.



References

- Ablain, M., Lalau, N., Meyssignac, B., Fraudeau, R., Barnoud, A., Dibarboure, G., Egido, A., and Donlon, C.: Benefits of a second tandem flight phase between two successive satellite altimetry missions for assessing instrumental stability, *Ocean Science*, 21, 343–358, <https://doi.org/10.5194/os-21-343-2025>, 2025.
- 305 AVISO/DUACS: SWOT Level-3 KaRIn Low Rate SSH Expert, <https://doi.org/10.24400/527896/A01-2023.018>, 2024.
- Clerc, S., Donlon, C., Borde, F., Lamquin, N., Hunt, S. E., Smith, D., McMillan, M., Mittaz, J., Woolliams, E., Hammond, M., Banks, C., Moreau, T., Picard, B., Raynal, M., Rieu, P., and Guérou, A.: Benefits and Lessons Learned from the Sentinel-3 Tandem Phase, *Remote Sensing*, 12, 2668, <https://doi.org/10.3390/rs12172668>, 2020.
- Cronin, M., Weller, R., Lampitt, R., and Send, U.: Ocean Reference Stations, in: *Earth Observation*, edited by Rustamov, R., InTech, ISBN 310 978-953-307-973-8, <https://doi.org/10.5772/27423>, 2012.
- Dibarboure, G., Pujol, M.-I., Briol, F., Traon, P. Y. L., Larnicol, G., Picot, N., Mertz, F., and Ablain, M.: Jason-2 in DUACS: Updated System Description, First Tandem Results and Impact on Processing and Products, *Marine Geodesy*, 34, 214–241, <https://doi.org/10.1080/01490419.2011.584826>, 2011.
- Dinardo, S., Maraldi, C., Daguze, J.-A., Amraoui, S., Boy, F., Moreau, T., and Picot, N.: Sentinel-6 MF Poseidon-4 Radar Altimeter In-Flight 315 Calibration and Performances Monitoring, <https://doi.org/10.24400/527896/A03-2022.3377>, publisher: CNES, 2022.
- Dorandeu, J., Ablain, M., Faugère, Y., Mertz, F., Soussi, B., and Vincent, P.: Jason-1 global statistical evaluation and performance assessment: Calibration and cross-calibration results, *Marine Geodesy*, 27, 345–372, <https://doi.org/10.1080/01490410490889094>, 2004.
- Dufau, C., Orsztynowicz, M., Dibarboure, G., Morrow, R., and Le Traon, P.: Mesoscale resolution capability of altimetry: Present and future, *Journal of Geophysical Research: Oceans*, 121, 4910–4927, <https://doi.org/10.1002/2015JC010904>, 2016.
- 320 European Space Agency: Copernicus Sentinel-3 Next Generation Topography Mission Requirements Document, Tech. rep., European Space Agency, <https://doi.org/10.5281/ZENODO.17454428>, version Number: 1.0, 2025.
- Guérou, A., Meyssignac, B., Prandi, P., Ablain, M., Ribes, A., and Bignalet-Cazalet, F.: Current observed global mean sea level rise and acceleration estimated from satellite altimetry and the associated measurement uncertainty, *Ocean Science*, 19, 431–451, <https://doi.org/10.5194/os-19-431-2023>, 2023.
- 325 Henry, O., Ablain, M., Meyssignac, B., Cazenave, A., Masters, D., Nerem, S., and Garric, G.: Effect of the processing methodology on satellite altimetry-based global mean sea level rise over the Jason-1 operating period, *Journal of Geodesy*, 88, 351–361, <https://doi.org/10.1007/s00190-013-0687-3>, 2014.
- LEULIETTE, E. W., NEREM, R. S., and MITCHUM, G. T.: Calibration of TOPEX/Poseidon and Jason Altimeter Data to Construct a Continuous Record of Mean Sea Level Change, *Marine Geodesy*, 27, 79–94, <https://doi.org/10.1080/01490410490465193>, publisher: 330 Taylor & Francis _eprint: <https://doi.org/10.1080/01490410490465193>, 2004.
- Masters, D., Nerem, R. S., Choe, C., Leuliette, E., Beckley, B., White, N., and Ablain, M.: Comparison of Global Mean Sea Level Time Series from TOPEX/Poseidon, Jason-1, and Jason-2, *Marine Geodesy*, 35, 20–41, <https://doi.org/10.1080/01490419.2012.717862>, 2012.
- Nilsson, J., Desai, S., Desjonquieres, J.-D., and Haines, B.: Global cross-calibration of the Jason-3 and Sentinel-6 Michael Freilich missions during their tandem period, <https://doi.org/10.24400/527896/A03-2022.3354>, publisher: CNES, 2022.
- 335 Prandi, P., Meyssignac, B., Ablain, M., Spada, G., Ribes, A., and Benveniste, J.: Local sea level trends, accelerations and uncertainties over 1993–2019, *Scientific Data*, 8, 1, <https://doi.org/10.1038/s41597-020-00786-7>, number: 1 Publisher: Nature Publishing Group, 2021.



Rieu, P., Moreau, T., Cadier, E., Raynal, M., Clerc, S., Donlon, C., Borde, F., Boy, F., and Maraldi, C.: Exploiting the Sentinel-3 tandem phase dataset and azimuth oversampling to better characterize the sensitivity of SAR altimeter sea surface height to long ocean waves, *Advances in Space Research*, 67, 253–265, <https://doi.org/10.1016/j.asr.2020.09.037>, 2021.

340 Zawadzki, L. and Ablain, M.: Accuracy of the mean sea level continuous record with future altimetric missions: Jason-3 vs. Sentinel-3a, *Ocean Sci.*, 12, 9–18, <https://doi.org/10.5194/os-12-9-2016>, 2016.

Zhao, Z.: Internal Tides From SWOT: A 75-Day Instantaneous Mode-1 M_2 Internal Tide Model, *Journal of Geophysical Research: Oceans*, 129, e2024JC021174, <https://doi.org/10.1029/2024JC021174>, 2024.

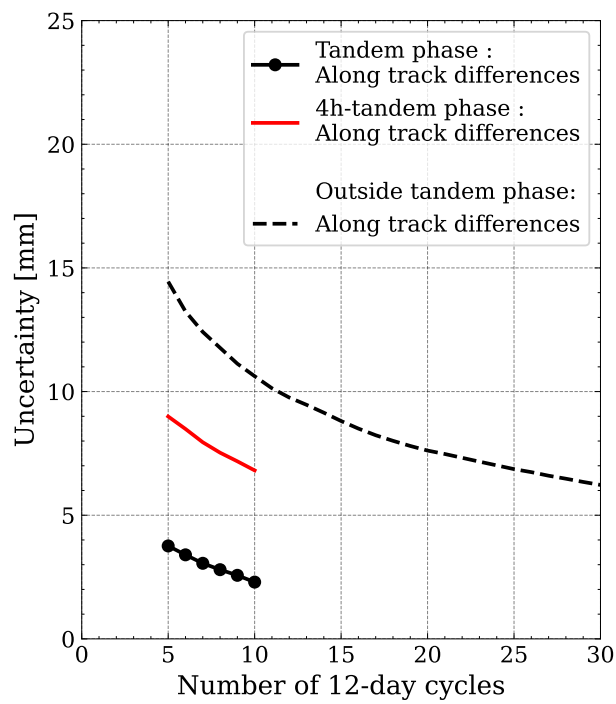


Figure 1. S3A and S3B regional offset uncertainties on 3x3° grid for 12-day subcycles, for along-track comparison methods with three different configurations: tandem phase, 4h-tandem phase, outside tandem phase.

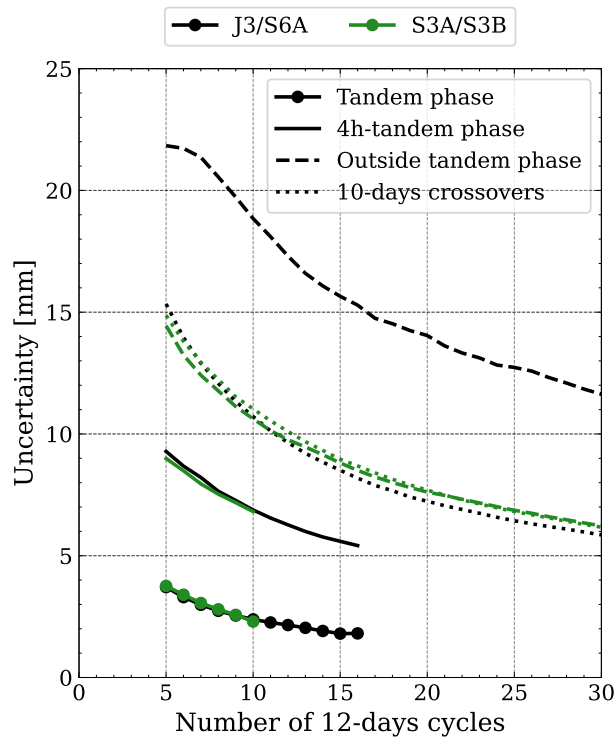


Figure 2. J3/S6A (black) and S3A/S3B (green) regional offset uncertainties on 3x3° grid for 12-day subcycles, for four different comparison methods: tandem phase, 4h-tandem phase, outside tandem phase and 10-days crossovers.

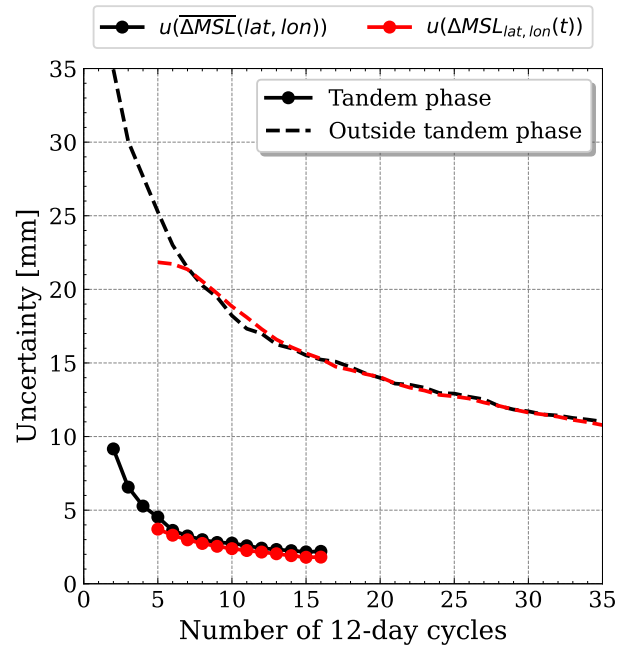


Figure 3. Comparison of two uncertainty estimation methods for J3/S6A in a regional analysis using a $3^\circ \times 3^\circ$ grid resolution.

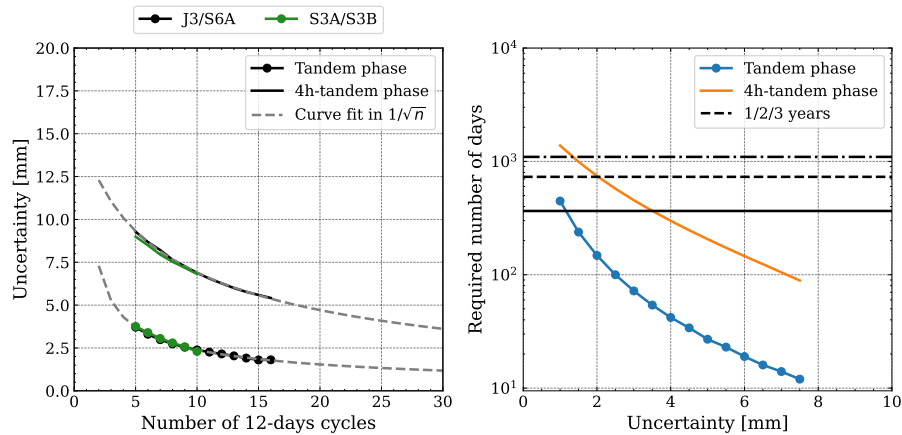


Figure 4. Use of the J3/S6A comparison during the tandem phase to fit the uncertainty evolution (left figure) and to estimate the number of days (right figure) required for the 4-hour tandem phase (orange) to reach the same precision as the classical tandem phase (blue). The horizontal black lines indicate, from bottom to top, the 1-, 2-, and 3-year thresholds.

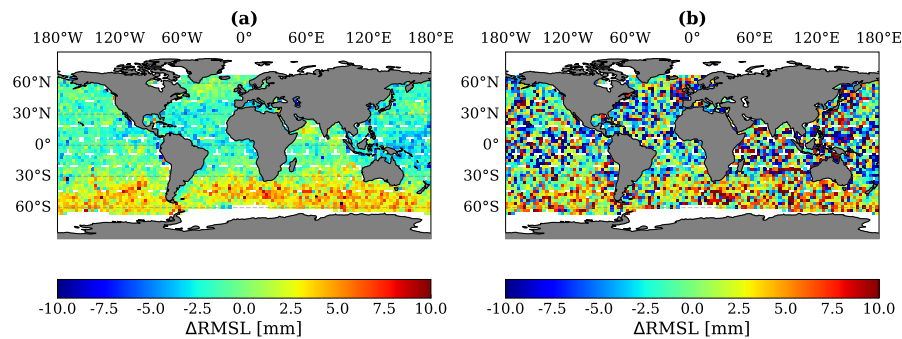


Figure A1. Differences between S3A and S3B for (a) Classical tandem phase for 3*3° boxes and (b) 4-hours tandem phase for 3*3° boxes

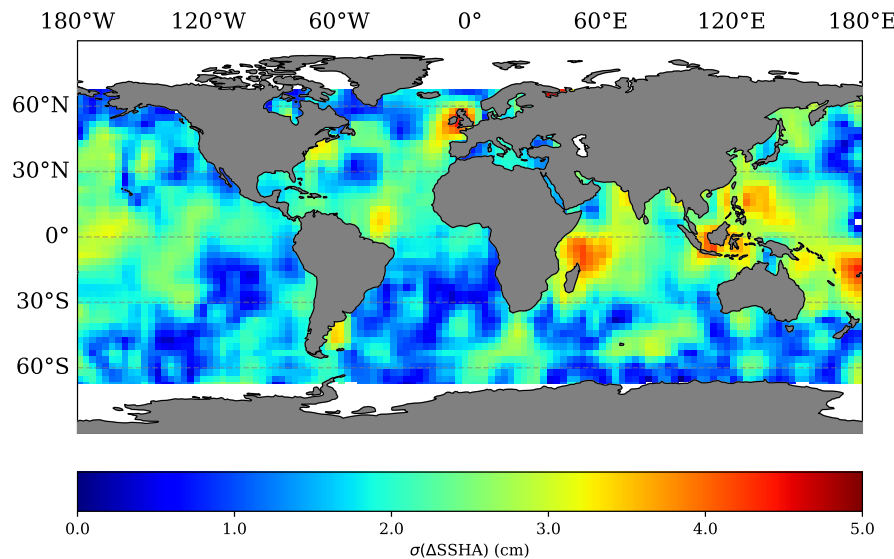


Figure A2. Map of variability in 4-hours time interval, from SWOT KaRIn and S3A and S3B crossovers.